

Glutamate and Aspartate as Proton Shuttles in Mutants of Carbonic Anhydrase[†]

Minzhang Qian,[‡] Chingkuang Tu,[‡] J. Nicole Earnhardt,[§] Philip J. Laipis,[§] and David N. Silverman^{*,‡}

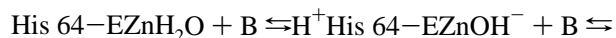
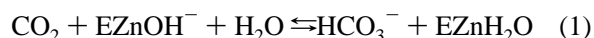
Department of Pharmacology and Therapeutics and Department of Biochemistry and Molecular Biology, University of Florida, Gainesville, Florida 32610-0267

Received August 21, 1997[®]

ABSTRACT: Maximal turnover rates for the hydration of CO₂ and the depletion of ¹⁸O from CO₂ catalyzed by carbonic anhydrase III (CA III) and carbonic anhydrase V (CA V) are limited by proton transfer involving zinc-bound water or hydroxide in the active site. We have investigated the capacity of glutamic and aspartic acids at position 64 in human CA III and murine CA V to act as proton shuttles in this pathway. The distance from the Cα of position 64 to the zinc is near 9.5 Å in the crystal structures of both CA III and CA V. Rates of intramolecular proton transfer between these proton shuttle groups and the zinc-bound water molecule were estimated as the predominant rate-contributing step in the catalytic turnover *k*_{cat} in the hydration of CO₂ measured by stopped flow and in the ¹⁸O exchange between CO₂ and water measured by mass spectrometry. We found that both glutamate and aspartate residues at position 64 are efficient proton shuttles in HCA III. The rate constant for intramolecular proton transfer from either residue to zinc-bound hydroxide is 4 × 10⁴ s⁻¹, about 20-fold greater than that of the wild type which has lysine at position 64. When the active site residue Phe 198 in human CA III was replaced with Leu, measurement of catalysis showed that Glu 64 retained but Asp 64 lost its capacity to act as a proton shuttle. These observations were supported in studies of catalysis by murine CA V which contains Leu 198; here again, Glu 64 acted as a proton shuttle, but Asp 64 did not. Phe 198 in HCA III is thus a significant factor in the capacity of the active site to sustain proton transfer, possibly through its stabilization of hydrogen-bonded water bridges that enhance proton translocation from both Glu and Asp at position 64 to the zinc-bound hydroxide.

Catalysis of the hydration of CO₂ by carbonic anhydrase has been useful in understanding the characteristics of proton transfer in enzymic systems. This catalysis occurs in two stages, the first of which is the conversion of CO₂ into HCO₃⁻ (eq 1) by direct nucleophilic attack of the zinc-bound hydroxide on CO₂ (1, 2). The second stage is the series of proton transfer steps that regenerates the zinc-bound hydroxide (eq 2). In these equations, B is buffer in solution and His 64 is the predominant proton shuttle group in carbonic anhydrase II (CA II¹) (3, 4). The imidazole ring of His 64 in CA II is within 8 Å of the zinc (5) and works as indicated in eq 2 to transfer a proton from the active site to buffer in solution. Since the distance between His 64 and the zinc-bound water is too long for direct proton transfer, there must be proton conduction along intervening water molecules; a network of hydrogen-bonded waters has been observed in the crystal structure (5, 6). This proton translocation mechanism is similar to proton conductance through

the gramicidin channel for which water chains form a proton wire (7, 8).



It is this second stage which is useful for the study of both inter- and intramolecular proton transfers (3, 9, 10).

Two isozymes of carbonic anhydrase which lack the His 64 proton shuttle have a maximal catalytic turnover in CO₂ hydration lower than that for CA II, in part because they lack an efficient mechanism for transferring protons to solution. Both murine CA V (MCA V) with Tyr 64 and human CA III (HCA III) with Lys 64 are slower carbonic anhydrases than CA II. In both cases, the side chains are too basic to serve as efficient proton shuttle residues at pH 6–8, and in both enzymes, the maximal velocity of catalysis can be increased by 10-fold or greater by placing a histidine at position 64 (11, 12). In all of these studies, intramolecular proton transfer between His 64 and the zinc-bound water has emerged as the predominant rate-contributing step of the maximal velocity in the range of pH 6–8, as determined by pH profiles, solvent hydrogen isotope effects, and chemical rescue of mutants lacking His 64.

Both murine CA V and bovine CA III are zinc metalloenzymes of about 30 kDa with very similar backbone conformations in their crystal structures (13, 14) and a 45% amino acid sequence identity. Carbonic anhydrase V is found primarily in liver mitochondria (15); CA III is a cytosolic enzyme present in skeletal muscle, fat, and liver (16, 17).

[†] This work was supported by Grant GM25154 from the National Institutes of Health.

* Address correspondence to Dr. David N. Silverman, Box 100267 Health Center, University of Florida College of Medicine, Gainesville, FL 32610-0267. Telephone: (352) 392-3556. Fax: (352) 392-9696. E-mail: silvrnm@nervm.nerdc.ufl.edu.

[‡] Department of Pharmacology and Therapeutics.

[§] Department of Biochemistry and Molecular Biology.

[®] Abstract published in *Advance ACS Abstracts*, November 15, 1997.

¹ Abbreviations: CA, carbonic anhydrase; MCA V, murine carbonic anhydrase V; Y64H CA V, mutant of CA V containing the replacement Tyr 64 → His; HCA III, human carbonic anhydrase III; Ches, 2-(*N*-cyclohexylamino)ethanesulfonic acid; Hepes, 4-(2-hydroxyethyl)-1-piperazineethanesulfonic acid; Mes, 2-(*N*-morpholino)ethanesulfonic acid; Mops, 3-(*N*-morpholino)propanesulfonic acid; Taps, 3-[[tris(hydroxymethyl)methyl]amino]propanesulfonic acid.

We have investigated the ability of glutamic or aspartic acid to act as a proton shuttle in catalysis by carbonic anhydrases III and V. These are neutral proton donors in contrast to the positively charged imidazolium of histidine, and they allow comparisons of proton transfer rates involving side chains of different lengths. We have found that glutamic acid at position 64 (K64E) and aspartic acid at position 64 (K64D) in HCA III have equivalent catalytic rate constants for intramolecular proton transfer. Since Glu 64 and Asp 64 do not have a similar range of side chain conformations, this result suggests that different pathways for proton transfer through hydrogen-bonded water exist in these two proteins. Analysis of additional mutants showed that the presence of phenylalanine at nearby position 198 in HCA III had a significant role in the ability of these residues to carry out proton transfer. With Leu at position 198, the active site lost the capability to utilize Asp 64 as a proton shuttle, a result confirmed in mutants of CA V. Since the conformation of the Asp 64 side chain and the formation of a hydrogen-bonded water structure are necessary for the translocation of protons, these results suggest Phe 198 has an effect in stabilizing such a water chain linking a productive conformation of Asp 64 to the zinc-bound water.

MATERIALS AND METHODS

Mutagenesis and Expression. The mouse CA V coding sequence was derived from BALB/C mouse liver mRNA by reverse transcription and PCR (18). All of the expressed mouse CA V utilized in this study was a truncated form lacking the first 51 amino terminal residues, which includes a mitochondrial leader sequence. In a numbering scheme consistent with CA II, the expressed CA V variants began at residue 22, Ser. This truncated form of CA V [denoted CA V_c by Heck et al. (18)] has been shown to have catalytic properties identical to those of CA V_a expressed from both a full length coding sequence and a 30-residue truncation of CA V_b (18). Mutant forms of CA V_c were created using a mutating oligonucleotide (19) in the pET31 expression vector system (20); alterations were verified by DNA sequencing. Wild type and mutant forms of the enzyme were expressed using the same pET vector, transformed into *Escherichia coli* BL21(DE3)pLysS (21). Protein expression levels ranged from 0.5 to 10 mg/L, depending on the mutant.

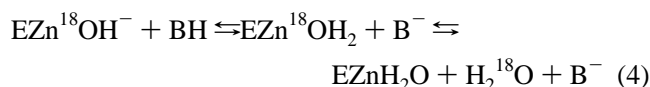
For human CA III and mutants, bacterial expression vectors optimized for efficient site-directed mutagenesis and protein synthesis were used, as described by Tanhauser et al. (20). The full length wild type and cassette mutants were prepared with these vectors with expression ranging from 1 to 20 mg/L, depending on the mutant. Again, all mutations were confirmed by DNA sequencing of the expression vector used to produce the mutant protein.

Purification. Procedures described by Heck et al. (18) were used to purify CA V and mutants. Frozen BL21(DE3)-pLysS cells expressing one of the mouse CA V variants were thawed in a solution of 100 mM Tris, 50 mM Na₂SO₄, 1 mM mercaptoethanol, 1 mM phenylmethanesulfonyl fluoride, 1 mM benzamidine, and 2 μM leupeptin at pH 9. This solution was stirred at 4 °C in the presence of 0.1 mg/mL deoxyribonuclease I for 1 h to allow the cells to lyse and to degrade the bacterial DNA. Cellular debris was removed by centrifugation, and recombinant CA V was purified from the resulting supernatant by affinity chromatography using

p-aminomethylbenzenesulfonamide coupled to agarose beads (22). The purity of the isolated enzymes was estimated at greater than 95% as determined by electrophoresis on a 10% polyacrylamide gel stained with Coomassie Blue. The concentration of each enzyme was determined from a Henderson plot (23) after titrating the active site with ethoxzolamide. The mutant Y64E/F65A MCA V was found to be unstable with a half-life of about 3 days when stored at 4 °C in 1 mM Tris buffer at pH 8.5. The mutant Y64D/F65A MCA V was also unstable under these conditions but with a half-life closer to 6 days.

Purification of HCA III and mutants was achieved by gel filtration followed by ion exchange chromatography as described by Tu et al. (24). The resulting enzymes were greater than 95% pure as determined by polyacrylamide gel electrophoresis. Concentrations of HCA III and mutants were determined from the molar absorptivity of $6.2 \times 10^4 \text{ M}^{-1} \text{ cm}^{-1}$ at 280 nm (25). Determination of the concentration of isozyme III and mutants with an inhibitor was not possible because it is relatively resistant to inhibition by sulfonamides.

¹⁸O Exchange. Mass spectrometry was used to measure the catalyzed and uncatalyzed rates of exchange of ¹⁸O from species of CO₂ into water and the rates of exchange of ¹⁸O between ¹²C-containing and ¹³C-containing species of CO₂ at chemical equilibrium. Equations 3 and 4 demonstrate the catalytic pathway for the exchange of ¹⁸O from bicarbonate to water. In eq 4, B⁻ is a buffer in solution and/or an amino acid side chain in the enzyme.



This method is capable of determining two rates in the catalytic pathway (26), as described below. The first is *R*₁, the rate of interconversion of CO₂ and HCO₃⁻ at chemical equilibrium. Equation 5 expresses the substrate dependence of *R*₁.

$$R_1/[E] = k_{\text{cat}}^{\text{ex}}[S]/(K_{\text{eff}}^S + [S]) \quad (5)$$

Here, [E] is the total enzyme concentration, *k*_{cat}^{ex} is a rate constant for maximal HCO₃⁻ to CO₂ interconversion, [S] is the substrate concentration of HCO₃⁻ and/or CO₂, and *K*_{eff}^S is an apparent substrate binding constant (27). This equation can be used to determine the values of *k*_{cat}^{ex}/*K*_{eff}^S when applied to the data for varying substrate concentrations or to determine *k*_{cat}^{ex}/*K*_{eff}^S directly from *R*₁ when [S] ≪ *K*_{eff}^S. In all of the studies reported here, the values of *R*₁/[E] as a function of total concentration of all species of CO₂ was linear up to ([CO₂] + [HCO₃⁻]) = 100 mM. This indicates that [S] ≪ *K*_{eff}^S, and under this condition, *k*_{cat}^{ex}/*K*_{eff}^S can be obtained directly from *R*₁/[E]. Under steady state conditions, when [S] ≪ *K*_m, all enzyme species are at their equilibrium concentrations. Hence, in both theory and practice, *k*_{cat}^{ex}/*K*_{eff}^{CO₂} is equivalent to *k*_{cat}/*K*_m for CO₂ hydration as measured by steady state methods (26, 27).

The second rate determined by this method is the rate of release from the enzyme of water labeled with ¹⁸O which is designated *R*_{H₂O} (eq 4). A proton donated from a donor

group BH converts the zinc-bound hydroxide to zinc-bound water, which readily exchanges with unlabeled water. The ^{18}O label is greatly diluted in the solvent water. The value of $R_{\text{H}_2\text{O}}$ can be interpreted in terms of the rate constant from a predominant donor group to the zinc-bound hydroxide according to eq 6 (28), in which k_{B} is the rate constant for proton transfer to the zinc-bound hydroxide, K_{B} is the ionization constant for the donor group, and K_{E} is the ionization constant of the zinc-bound water molecule.

$$R_{\text{H}_2\text{O}}/[E] = k_{\text{B}}/[(1 + K_{\text{B}}/[H^+])(1 + [H^+]/K_{\text{E}})] \quad (6)$$

An Extrel EMX-200 mass spectrometer and a membrane inlet permeable to dissolved gases was used to measure the rate of distribution of ^{18}O (26). Unless otherwise indicated, experiments were carried out in the absence of buffers which were not needed to maintain pH since these experiments were carried out at chemical equilibrium.

Steady State Constants. Initial velocities of the hydration of CO_2 were measured with a stopped-flow spectrophotometer (Applied Photophysics model SF.17MV); since this catalysis produces protons as well as HCO_3^- , we measured the initial rate of hydration by recording the absorbance change of a pH indicator (29). Saturated CO_2 solutions were made by bubbling CO_2 into water at 25 °C. Syringes with gastight seals were used to make CO_2 dilutions from 17 to 0.43 mM. The pK_{a} of the buffer indicator pairs, and the observed wavelengths, were as follows: Mes ($\text{pK}_{\text{a}} = 6.1$) and chlorophenol red ($\text{pK}_{\text{a}} = 6.3$, 574 nm), Mops ($\text{pK}_{\text{a}} = 7.2$) with *p*-nitrophenol ($\text{pK}_{\text{a}} = 7.1$, 400 nm), Hepes ($\text{pK}_{\text{a}} = 7.5$) with phenol red ($\text{pK}_{\text{a}} = 7.5$, 557 nm), Taps ($\text{pK}_{\text{a}} = 8.4$) with *m*-cresol purple ($\text{pK}_{\text{a}} = 8.3$, 578 nm), Ches ($\text{pK}_{\text{a}} = 9.3$), and thymol blue ($\text{pK}_{\text{a}} = 8.9$, 590 nm). The buffer concentrations were 25 mM, unless otherwise indicated, and the total ionic strength for each buffer–indicator pair system was maintained at 0.1 M by the addition of the appropriate amount of Na_2SO_4 . The mean of four to eight reaction traces of the first 5–10% of the reaction was used to determine initial rates. The uncatalyzed rates were subtracted and the rate constants k_{cat} and $k_{\text{cat}}/K_{\text{m}}$ determined by nonlinear least-squares methods (Enzfitter, Elsevier-Biosoft).

RESULTS

To determine the rates of intramolecular proton transfer between amino acid residues acting as proton shuttle groups and the zinc-bound water, we have determined rate constants for catalysis by two methods: measurements of initial velocities of CO_2 hydration at steady state by stopped-flow spectrophotometry and measurements of ^{18}O exchange between CO_2 and water at chemical equilibrium by mass spectrometry.

Human CA III. Our measurements of $k_{\text{cat}}/K_{\text{m}}$ for wild type HCA III gave a maximal value near $6 \times 10^5 \text{ M}^{-1} \text{ s}^{-1}$ (Table 1). The two mutants K64E HCA III and K64D HCA III were very similar with maximal values of $k_{\text{cat}}/K_{\text{m}}$ also near $6 \times 10^5 \text{ M}^{-1} \text{ s}^{-1}$. The ratio $k_{\text{cat}}/K_{\text{m}}$ contains rate constants for the steps in the interconversion of CO_2 and HCO_3^- (eq 1) and not the subsequent proton transfer steps (eq 2). These similar values of $k_{\text{cat}}/K_{\text{m}}$ are useful as a control indicating that the mutations at residue 64 have not altered the rates of

Table 1: Maximal Values of $k_{\text{cat}}/K_{\text{m}}$ and k_{cat} and the Apparent Values of pK_{a} Determined from pH Profiles for Catalysis of CO_2 Hydration by Murine CA V and Mutants and Human CA III and Mutants^a

enzyme	$k_{\text{cat}}/K_{\text{m}}$ ($\times 10^5 \text{ M}^{-1} \text{ s}^{-1}$)	$\text{pK}_{\text{a}}(k_{\text{cat}}/K_{\text{m}})^b$	k_{cat} ($\times 10^4 \text{ s}^{-1}$)	$\text{pK}_{\text{a}}(k_{\text{cat}})^b$
wild type HCA III ^c	6.7 ± 0.3	5.3 ± 0.2	0.2	not pH-dependent
K64E HCA III	6.2 ± 0.1	5.3 ± 0.1	1.0	8.5 ± 0.5
K64D HCA III	7.2 ± 0.1	5.5 ± 0.1	3.7 ± 1.5	<6
K64E/F198L HCA III	67 ± 2	6.1 ± 0.1	6.9 ± 0.6	<6
K64D/F198L HCA III	69 ± 3	6.0 ± 0.1	1.3 ± 0.2	<6
wild type MCA V	1.1 ± 0.1	7.3 ± 0.1	3.2 ± 0.2^d	9.2 ± 0.1^d
Y64E/F65A MCA V	1.6 ± 0.1	7.7 ± 0.1	>1	>9.3
Y64D/F65A MCA V	1.2 ± 0.1	6.8 ± 0.1	0.11 ± 0.01	<6
			5.2 ± 0.6	9.3 ± 0.2

^a The values of $k_{\text{cat}}/K_{\text{m}}$ for MCA V and its mutants were measured at 10 °C. All other data were obtained at 25 °C. Values of $k_{\text{cat}}/K_{\text{m}}$ were obtained from ^{18}O exchange measurements and values of k_{cat} from stopped-flow spectrophotometry. These maxima and apparent values of pK_{a} were calculated from the best fit to a single ionization or to the sum of two ionizations by least-squares analysis. ^b These are apparent pK_{a} values determined from $k_{\text{cat}}/K_{\text{m}}$ and k_{cat} . The standard errors of these parameters resulted from least-squares fits to the data; errors of less than 0.1 were rounded off to 0.1. ^c These data are from Jewell et al. (11). ^d These data are from Heck et al. (12, 18) at 25 °C.

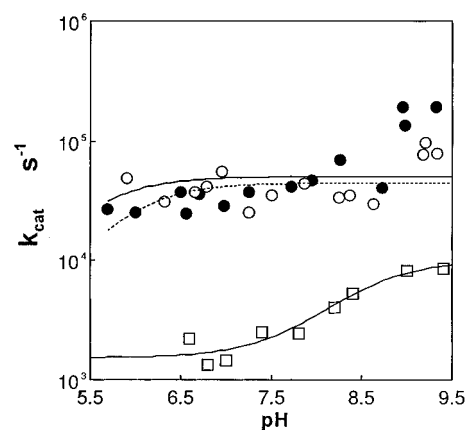


FIGURE 1: Turnover number k_{cat} for the hydration of CO_2 catalyzed by (□) wild type human CA III, (○) the mutant human K64E CA III, and (●) the mutant human K64D CA III. Data were obtained at 25 °C by stopped-flow spectrophotometry using solutions containing the following buffers at 25 mM: pH 5.8–6.9, Mes; pH 6.6–7.3, Mops; pH 7.1–7.9, Hepes; pH 8.1–8.7, Taps; and pH >8.9, Ches. Maximal values of k_{cat} are given in Table 1. The data for the wild type enzyme are from Jewell et al. (11).

interconversion of CO_2 and HCO_3^- and hence have caused no significant structural changes that would affect the first stage of catalysis.

The values of k_{cat} for CO_2 hydration catalyzed by the mutants K64E and K64D HCA III, determined by stopped flow, were similar and independent of pH at k_{cat} near $4 \times 10^4 \text{ s}^{-1}$. This is 20-fold greater than the k_{cat} for wild type HCA III which is $2 \times 10^3 \text{ s}^{-1}$ at pH <8 (Figure 1, Table 1). Such an enhancement is consistent with proton transfer from Glu 64 and Asp 64.

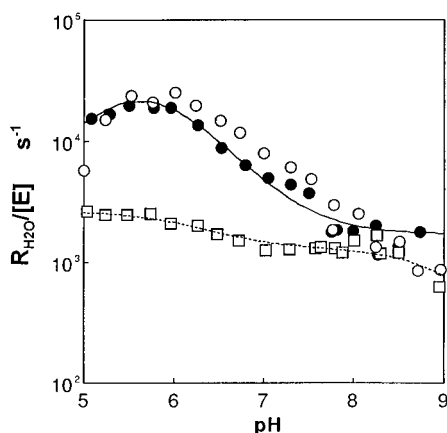


FIGURE 2: Rate constants for the release of ^{18}O -labeled water, $R_{\text{H}_2\text{O}}/[\text{E}]$, from the active sites of (\square) wild type human CA III, (\circ) the mutant human K64E CA III, and (\bullet) the mutant human K64D CA III. Data were measured at 25 °C in solutions containing no buffers. The total concentration of all species of CO_2 was 25 mM. The total ionic strength of solution was maintained at 0.2 by addition of Na_2SO_4 . The lines are least-squares fits to eq 6 with the constants given in Table 2.

Table 2: Rate Constants k_B for Proton Transfer from Donor Groups to Zinc-Bound Hydroxide in Murine CA V and Human CA III and Mutants^a

enzyme	$\text{pK}_a(\text{ZnH}_2\text{O})$	$\text{pK}_a(\text{donor})$	$k_B (\times 10^{-4} \text{ s}^{-1})$
wild type HCA III ^b	<5	>9	0.2–0.3
K64E HCA III	5.3 ± 0.2	6.4 ± 0.3	3.8 ± 0.8
K64D HCA III	~ 5.5	5.7 ± 0.2	5.7 ± 0.3
K64A HCA III	<5	>9	0.2–0.3
K64E/F198L HCA III	5.8 ± 0.2	5.8 ± 0.2	4.8 ± 1.9
K64D/F198L HCA III	not pH-dependent		0.9 ± 0.2
F198L HCA III ^c	not pH-dependent		1.0 ± 0.2
wild type MCA V	7.4 ± 0.1	8.8 ± 0.2	4.0 ± 0.6
Y64E/F65A MCA V	8.1 ± 0.3	5.4 ± 0.3	1.8
Y64D/F65A MCA V	7.1 ± 0.1	>9	>2
F65A MCA V	7.0 ± 0.1	8.7 ± 0.1	4.4 ± 0.5

^a These constants and values of the pK_a of the donor and acceptor groups were estimated from the rates of release of H_2^{18}O from the enzymes using eq 6. The data for MCA V and its mutants were obtained at 10 °C and the data for HCA III at 25 °C. Experimental conditions were as described in the legend to Figure 2 for HCA III and in the legend to Figure 5 for MCA V. ^b Data from Jewell et al. (11). ^c Data from LoGrasso et al. (30).

The proton transfer-dependent rate constant $R_{\text{H}_2\text{O}}/[\text{E}]$ for release of H_2^{18}O from wild type HCA III was rather independent of pH, with a value near $2 \times 10^3 \text{ s}^{-1}$ (Figure 2). The values of $R_{\text{H}_2\text{O}}/[\text{E}]$ for the mutants K64E HCA III and K64D HCA III were very similar to each other. They appeared to resemble that for wild type at $\text{pH} > 7.5$ with a plateau at about $2 \times 10^3 \text{ s}^{-1}$ (Figure 2). At $\text{pH} < 7.5$, we observed a bell-shaped pH dependence for $R_{\text{H}_2\text{O}}/[\text{E}]$ with a maximum near $\text{pH} 5.8$ (Figure 2), consistent with a proton donor with a pK_a near 6 and a pK_a near 5.5 for the conjugate acid of the proton acceptor, the zinc-bound hydroxide (Table 2). These bell-shaped values of $R_{\text{H}_2\text{O}}/[\text{E}]$ describe the proton transfer roles of Glu 64 and Asp 64, and appear to be superimposed on or added to the base value for $R_{\text{H}_2\text{O}}/[\text{E}]$ of $2 \times 10^3 \text{ s}^{-1}$. The values of k_B , a rate constant for

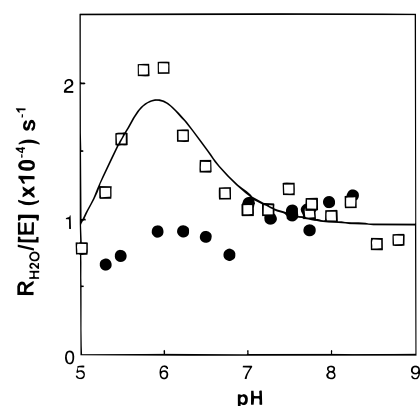


FIGURE 3: Rate constants for the release of ^{18}O -labeled water, $R_{\text{H}_2\text{O}}/[\text{E}]$, from the active sites of (\square) K64E/F198L human CA III and (\bullet) K64D/F198L human CA III. Data were measured at 25 °C in solutions containing no buffers. The total concentration of all species of CO_2 was 25 mM. The ionic strength of solution was maintained at 0.2 by addition of Na_2SO_4 .

intramolecular proton transfer, obtained from these data using eq 6 were near $4\text{--}6 \times 10^4 \text{ s}^{-1}$ (Table 2).

The experiments described above showed that single-site mutants of HCA III with Glu or Asp at residue 64 had nearly equivalent catalytic activity. We found a different result with murine CA V (described below). To make the active site of CA III more like that of CA V, we replaced Phe 198 in CA III with Leu and took the following data. Measurements of $R_{\text{H}_2\text{O}}/[\text{E}]$ were carried out on two additional mutants, K64D/F198L and K64E/F198L HCA III. In this case, $R_{\text{H}_2\text{O}}/[\text{E}]$ for K64D/F198L (Figure 3) was very similar to that observed for the single mutant F198L [Figure 2 of LoGrasso et al. (30)], showing no pH dependence with a value of $R_{\text{H}_2\text{O}}/[\text{E}]$ near 10^4 s^{-1} . The data for K64E/F198L showed evidence of the bell-shaped pH dependence (Figure 3) seen also for the single mutants K64E and K64D HCA III, with pertinent constants given in Table 2. This bell-shaped display for K64E/F198L was also observed in four other experiments where the temperature was changed to 10 °C and the total substrate concentration of all species of CO_2 to 5 mM. The comparison of the values of k_{cat}/K_m showed no significant differences between K64D/F198L and K64E/F198L HCA III (Table 1). However, the values of k_{cat} (Table 1) confirmed enhanced activity for the mutant K64E/F198L HCA III. Hence, Glu 64 in K64E/F198L HCA III appears to function as a proton shuttle, but Asp 64 in K64D/F198L does not.

Murine CA V. The mutants of CA V we studied have Asp or Glu at residue 64 and also Ala at 65. The choice of these double mutants is based on the observations (12, 13) that the presence of Phe 65 in CA V limits the mobility and forces an outward conformation of the side chains of Tyr 64 and His 64, minimizing the role of His 64 as a proton shuttle in Y64H MCA V. To remove the effect of this residue on the proton shuttle capacity of Asp 64 or Glu 64, we have mutated Phe 65 to Ala. The values of k_{cat}/K_m for wild type MCA V and the two mutants Y64E/F65A and Y64D/F65A MCA V were very similar over the pH range from 5 to 9, each enzyme achieving a maximum very near $k_{\text{cat}}/K_m = 1 \times 10^7 \text{ M}^{-1} \text{ s}^{-1}$ (Table 1). Again, these results serve as a control and indicate that the replacements at positions 64 and 65 have little effect on the first stage of catalysis (eq 1).

The values of k_{cat} for wild type MCA V and for the mutant Y64D/F65A MCA V were similar, with a maximum near

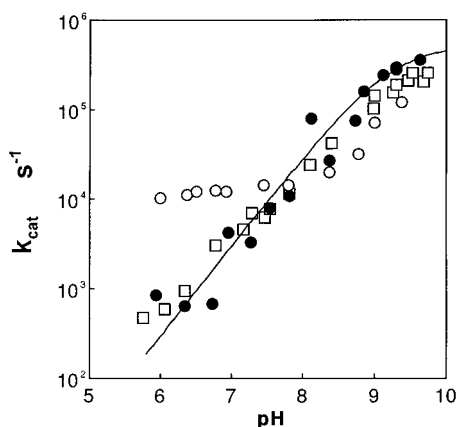


FIGURE 4: Turnover number k_{cat} for the hydration of CO_2 catalyzed by (□) wild type murine CA V, (○) the mutant murine Y64E/F65A CA V, and (●) the mutant murine Y64D/F65A CA V. Data were obtained at 25 °C by stopped-flow spectrophotometry using solutions containing the following buffers at 25 mM: pH 5.8–6.9, Mes; pH 6.6–7.3, Mops; pH 7.1–7.9, Hepes; pH 8.1–8.7, Taps; and pH >8.9, Ches. The line is a least-squares fit of the data to one ionization for Y64D/F65A CA V with values given in Table 1.

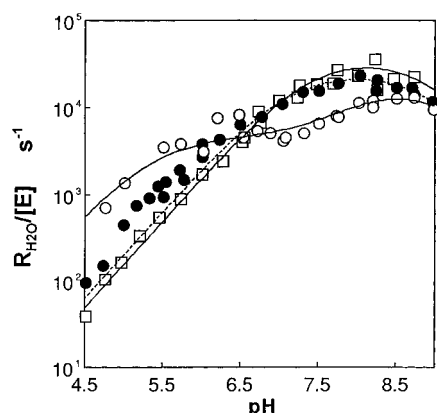


FIGURE 5: Rate constants for the release of ^{18}O -labeled water, $R_{\text{H}_2\text{O}}/[\text{E}]$, from the active sites of (□) wild type murine CA V, (○) the mutant murine Y64E/F65A CA V, and (●) the mutant murine Y64D/F65A CA V. Data were measured at 10 °C in solutions containing no buffers. The total concentration of all species of CO_2 was 25 mM. The total ionic strength of solution was maintained at 0.2 by addition of Na_2SO_4 . The lines are least-squares fits to eq 6 with the constants given in Table 2.

$3\text{--}5 \times 10^5 \text{ s}^{-1}$ at high pH and an apparent pK_a near 9.2 (Figure 4, Table 1). However, the values of k_{cat} for the mutant Y64E/F65A MCA V, although similar at pH >8, formed a plateau at $k_{\text{cat}} = 10^4 \text{ s}^{-1}$ at pH <8, consistent with its role as a proton acceptor with a pK_a of <6. The results for $R_{\text{H}_2\text{O}}/[\text{E}]$ (Figure 5) were similar to those for k_{cat} ; the values of $R_{\text{H}_2\text{O}}/[\text{E}]$ for the wild type and the mutant Y64D/F65A MCA V were nearly identical, while those for Y64E/F65A MCA V in the lower-pH region were somewhat larger than those of the other two forms. The data for $R_{\text{H}_2\text{O}}/[\text{E}]$ were fit to the sum of two ionizations (as given in eq 6) describing the proton donor and acceptor with the constants given in Table 2. The values of pK_a for the zinc-bound water (determined from $R_{\text{H}_2\text{O}}/[\text{E}]$, Table 2) were similar to those obtained from k_{cat}/K_m (Table 1).

DISCUSSION

CA III and Mutants. The catalytic turnover k_{cat} for hydration of CO_2 catalyzed by wild type HCA III, with

values near $2 \times 10^3 \text{ s}^{-1}$ (pH <8) (Figure 1), has been interpreted as being dominated by proton transfer to a weak proton acceptor of the enzyme or possibly to water with the emergence of a more efficient proton acceptor at pH >8 (11). Substitution of either aspartate or glutamate at position 64 leads to enhanced proton transfer. The turnover numbers k_{cat} for the mutants K64E and K64D appeared to be identical, with values near $4 \times 10^4 \text{ s}^{-1}$ (Figure 1, Table 1). Moreover, the lack of pH dependence for k_{cat} with these two mutants is consistent with either Glu or Asp enhancing catalysis by acting as proton acceptors with a pK_a of <5.5.

The similar values of k_{cat} suggest that both Asp 64 and Glu 64 are proton shuttles with similar efficiencies in these mutants of HCA III. This interpretation was supported by ^{18}O exchange data. $R_{\text{H}_2\text{O}}/[\text{E}]$ is a rate constant for the release of ^{18}O -labeled water from the enzyme (eq 4), and is limited in rate by proton transfer in the dehydration direction as determined by solvent hydrogen isotope effects, pH profiles, and chemical rescue (11). Both K64E and K64D variants displayed enhanced values of $R_{\text{H}_2\text{O}}/[\text{E}]$ at pH <8 with a bell-shaped pH dependency that could be used to estimate a pK_a of the proton donor group, Asp 64 or Glu 64, at a pK_a near 6 and the pK_a for the zinc-bound water near or less than 5.5 (Table 2, Figure 2). A similar pK_a of 5.6 for Glu 64 in H64E HCA II was suggested by the catalysis of the hydrolysis of 4-nitrophenyl acetate (31). Our results also estimate the rate constant for intramolecular proton transfer k_B from these carboxylic acids to the zinc-bound hydroxide molecule to be $4\text{--}6 \times 10^4 \text{ s}^{-1}$ (Table 2).² This value is about 2-fold greater than the rate constant for proton transfer from His 64 to zinc-bound hydroxide in K64H HCA III at $2 \times 10^4 \text{ s}^{-1}$ (28) and about 20-fold greater than in the wild type HCA III (at pH <8).

The data confirm that, despite the difference in the lengths of their side chains, Asp 64 in K64D participates in this intramolecular proton transfer to the same extent as does Glu 64 in K64E HCA III. Glutamic acid in an extended side chain conformation has a length from its $\text{C}\alpha$ to the proton donation site $\text{O}\epsilon$ (4.9 Å) which is very close to that of histidine from its $\text{C}\alpha$ to the proton donation site $\text{N}\epsilon$ (4.6 Å) when extended in a similar manner. On the other hand, this distance for Asp 64 is shorter by one methylene group ($\sim 0.8\text{--}1.2 \text{ Å}$). It is unlikely that Glu 64 and Asp 64 attain conformations in the transition state for proton transfer with their donating carboxylic acid groups equidistant from the zinc. It is more likely that there are a number of proton conduction pathways through different although short-lived structures of intervening water chains; the predominant conduction pathways for Asp 64 and Glu 64 might be different yet permit equivalent proton transfer rates.

CA V and Mutants. The pH profiles for k_{cat} for hydration catalyzed by wild type CA V and the mutant Y64D/F65A are similar throughout the pH range of 6–10 (Figure 4). This result indicates that Asp at position 64 has no detectable role as a proton shuttle. However, the pH dependence of k_{cat} for the mutant Y64E/F65A showed a plateau in the range of

² The rate constants for maximal turnover in hydration k_{cat} (Table 1) and intramolecular proton transfer k_B accompanying dehydration (Table 2) for the K64E and K64D mutants of HCA III are approximately equal ($\sim 4 \times 10^4 \text{ s}^{-1}$). This is expected since the pK_a values of both the carboxylic acid donors and the conjugate acid of the zinc-bound hydroxide acceptor group are similar (5–6).

pH <7.5 at a k_{cat} value of 10^4 s^{-1} . The plateau for this mutant is consistent with a proton shuttle role for Glu 64 with a value for $\text{p}K_{\text{a}}$ of <6. Such a result is also consistent with the data of Engstrand et al. (32), who observed a similar plateau at k_{cat} near $4 \times 10^4 \text{ s}^{-1}$ for H64E HCA II. Both the magnitude and the lack of pH dependence are also similar to that observed for k_{cat} in the mutant K64E of HCA III (Figure 1). Thus, the steady state data indicate a proton transfer role for Glu 64 in Y64E/F65A but no measurable role for Asp 64 in Y64D/F65A.

The pH profiles for $R_{\text{H}_2\text{O}}/[\text{E}]$, the rate of release of H_2^{18}O from the enzymes, confirm this conclusion. The pH profile for Y64E/F65A was higher in the pH range of <6 with values greater by as much as 7-fold than those with the wild type or Y64D/F65A (Figure 5). In the fit of eq 6 to the data for Y64E/F65A, a very approximate value of $\text{p}K_{\text{a}}$ near 5.4 was obtained for a proton donor with a rate constant for intramolecular proton transfer to the zinc-bound hydroxide of $1.8 \times 10^4 \text{ s}^{-1}$ (Table 2). These data are consistent with Glu 64 acting as a proton donor providing an effective proton shuttle in the pH region of below 7.5. The values of $R_{\text{H}_2\text{O}}/[\text{E}]$ were very similar when catalyzed by wild type CA V and Y64D/F65A (Figure 5). A fit of eq 6 to these results is consistent with a proton shuttle with a $\text{p}K_{\text{a}}$ near 9 and the zinc-bound water with a $\text{p}K_{\text{a}}$ near 7 (Table 2). The identity of the additional residues acting as proton shuttles with a $\text{p}K_{\text{a}}$ near 9 in MCA V is under current investigation. Thus, Asp 64 in Y64D/F65A MCA V has very small if any detectable proton shuttle capacity.

Effect of Nearby Residues. Our observations indicate that Asp 64 can act as a proton shuttle in K64D CA III but not in Y64D/F65A CA V. To explain this difference, we considered nearby residues in the active site cavity. A predominant difference is found at position 198 which is Phe in HCA III and is Leu in CA V and in CA II. Phe 198 is located on the hydrophobic side of the active site cavity of CA III with its ring (C δ) as close as 6.5 Å from the zinc; Lys 64 is on the hydrophilic side with its C α 12 Å from the ring (C δ) of Phe 198 in bovine CA III (14). Figure 3 shows that the double replacement Phe 198 \rightarrow Leu along with either Lys 64 \rightarrow Glu or Lys 64 \rightarrow Asp in HCA III gives proton transfer results for HCA III that now are similar to those for CA V. Glu 64 in the double mutant K64E/F198L is a proton shuttle with a bell-shaped pH dependence and enhanced values of $R_{\text{H}_2\text{O}}/[\text{E}]$. However, there is no detectable proton transfer from Asp 64 in K64D/F198L which lacks these features. The values of $R_{\text{H}_2\text{O}}/[\text{E}]$ for K64D/F198L HCA III are similar to those of the single mutant F198L HCA III (30). The results for k_{cat} (Table 1) also show enhanced activity for K64E/F198L compared with that for K64D/F198L.

An explanation for the enhancement of proton transfer we have observed with HCA III variants containing Phe 198 is that the presence of Phe 198 enhances proton transfer because of its effect on water structure in the active site. The side chains of residues 64 and 198 are too distant for a direct steric interaction; the hydrophobic side chain of Phe 198 is expected to be immobilized onto the hydrophobic surface of the active site cavity. Pomès and Roux (8) in modeling the water channel in gramicidin have concluded that the formation and breaking of hydrogen bonds within the water chain is the limiting process in proton translocation through the channel. This is also a conclusion that results from the

application of Marcus rate theory to intramolecular proton transfer in CA III (28). The present results suggest that the hydrophobic group Phe 198 in CA III stabilizes one or more water chains that promote proton transfer from Asp 64 to the zinc-bound hydroxide. Eriksson and Liljas (14) have detected a water molecule (number 335) in the crystal structure of bovine CA III that is hydrogen bonded to the π -electron system of the benzene ring of Phe 198. This water then forms a hydrogen bond to another water in the active site cavity (number 336) which in turn forms part of the hydrogen bonding scheme of water molecules in the active site cavity. This would suggest a stabilization of active site water structures in the mutant of CA III containing Phe 198 compared with that containing Leu 198, making the proton transfer rate more rapid for the mutant containing Asp 64/Phe 198 compared with Asp 64/Leu 198. This is an interesting contrast to the results of Jackman et al. (33) and Scolnick and Christianson (6), who observed the disruption of the active site solvent network and corresponding decrease in catalytic activity caused by making replacements at position 65 in HCA II; this site is adjacent to the proton shuttle residue His 64. In their studies, Leu 65 and Phe 65 were both among the bulky residues that when placed at position 65 caused such a decrease in activity. As would be expected, Phe with a larger side chain volume caused a greater decrease in activity than did Leu, although both substitutions were disruptive to active site water structure.

Conclusions. (1) Glutamate 64 can act as a proton shuttle residue in CA III with efficiency comparable to that for histidine at this position. (2) Aspartate 64 in CAIII is a proton shuttle with efficiency equivalent to that of Glu 64. Because of their different range of side chain conformations, this result suggests the presence of multiple pathways of proton transfer through intervening water molecules. (3)-The presence of Phe 198, compared with Leu 198, enhanced the efficiency of Asp 64 as a proton shuttle. This result was confirmed in CA V which naturally occurs with Leu 198. The property of Phe 198 that enhances the capability of Asp 64 to act as a proton shuttle is very likely related to its effect on the structure of active site water.

ACKNOWLEDGMENT

We thank Kevin Lentz, Yang Wang, and Yanping Zhang for excellent technical assistance.

REFERENCES

1. Christianson, D. W., and Fierke, C. A. (1996) *Acc. Chem. Res.* 29, 331–339.
2. Silverman, D. N., and Lindskog S. (1988) *Acc. Chem. Res.* 21, 30–36.
3. Steiner, H., Jonsson, B.-H., and Lindskog, S. (1975) *Eur. J. Biochem.* 59, 253–259.
4. Tu, C. K., Silverman, D. N., Forsman, C., Jonsson, B. H., and Lindskog, S. (1989) *Biochemistry* 28, 7913–7918.
5. Eriksson, A. E., Jones, T. A., and Liljas, A. (1988) *Proteins: Struct., Funct., Genet.* 4, 274–282.
6. Scolnick, L. R., and Christianson, D. W. (1996) *Biochemistry* 35, 16429–16434.
7. Nagle, J. F., and Morowitz, H. J. (1978) *Proc. Natl. Acad. Sci. U.S.A.* 75, 298–302.
8. Pomès, R., and Roux, B. (1996) *Biophys. J.* 71, 19–39.
9. Pocker, Y., Janjic, N., and Miao, C. H. (1986) in *Zinc Enzymes* (Bertini, I., Luchinat, C., Maret, W., and Zeppezauer, M., Eds.) pp 341–356, Birkhauser, Boston.

10. Rowlett, R. S., and Silverman, D. N. (1982) *J. Am. Chem. Soc.* **104**, 6737–6741.
11. Jewell, D. A., Tu, C. K., Paranawithana, S. R., Tanhauser, S. M., LoGrasso, P. V., Laipis, P. J., and Silverman, D. N. (1991) *Biochemistry* **30**, 1484–1490.
12. Heck, R. W., Boriack-Sjodin, P. A., Qian, M., Tu, C. K., Christianson, D. W., Laipis, P. J., and Silverman, D. N. (1996) *Biochemistry* **35**, 11605–11611.
13. Boriack-Sjodin, P. A., Heck, R. W., Laipis, P. J., Silverman, D. N., and Christianson, D. W. (1995) *Proc. Natl. Acad. Sci. U.S.A.* **92**, 10949–10953.
14. Eriksson, A. E., and Liljas, A. (1993) *Proteins: Struct., Funct., Genet.* **16**, 29–42.
15. Dodgson, S. J. (1991) in *The Carbonic Anhydrases* (Dodgson, S. J., Tashian, R. E., Gros, G., and Carter, N. D., Eds.) pp 297–306, Plenum Press, New York.
16. Geers, C., and Gross, G. (1991) in *The Carbonic Anhydrases* (Dodgson, S. J., Tashian, R. E., Gros, G., and Carter, N. D., Eds.) pp 227–240, Plenum Press, New York.
17. Lynch, C. J., Brennen, W. A., Vary, T. C., Carter, N., and Dodgson, S. J. (1993) *Am. J. Physiol.* **264**, E621–E630.
18. Heck, R. W., Tanhauser, S. M., Manda, R., Tu, C. K., Laipis, P. J., and Silverman, D. N. (1994) *J. Biol. Chem.* **269**, 24742–24746.
19. Kunkel, T. (1985) *Proc. Natl. Acad. Sci. U.S.A.* **82**, 488–492.
20. Tanhauser, S. M., Jewell, D. A., Tu, C. K., Silverman, D. N., and Laipis, P. J. (1992) *Gene* **117**, 113–117.
21. Studier, F. W., Rosenberg, A. H., Dunn, J. J., and Dubendorf, J. W. (1990) *Methods Enzymol.* **185**, 60–89.
22. Khalifah, R. G., Strader, D. J., Bryant, S. H., and Gibson, S. M. (1977) *Biochemistry* **16**, 2241–2247.
23. Segel, I. H. (1975) *Enzyme Kinetics*, pp 150–159, John Wiley & Sons, New York.
24. Tu, C. K., Thomas, H. G., Wynns, G. C., and Silverman, D. N. (1986) *J. Biol. Chem.* **261**, 10100–10103.
25. Engberg, P., Millqvist, E., Pohl, G., and Lindskog, S. (1985) *Arch. Biochem. Biophys.* **241**, 628–638.
26. Silverman, D. N. (1982) *Methods Enzymol.* **87**, 732–752.
27. Simonsson, I., Jonsson, B.-H., and Lindskog, S. (1979) *Eur. J. Biochem.* **93**, 409–417.
28. Silverman, D. N., Tu, C. K., Chen, X., Tanhauser, S. M., Kresge, A. J., and Laipis, P. J. (1993) *Biochemistry* **32**, 10757–10762.
29. Khalifah, R. G. (1971) *J. Biol. Chem.* **246**, 2561–2573.
30. LoGrasso, P. V., Tu, C. K., Jewell, D. A., Wynns, G. C., Laipis, P. J., and Silverman, D. N. (1991) *Biochemistry* **30**, 8463–8470.
31. Forsman, C., Behravan, G., Jonsson, B.-H., Liang, Z.-W., Lindskog, S., Ren, X., Sandstrom, J., and Wallgren, K. (1988) *FEBS Lett.* **229**, 360–362.
32. Engstrand, C., Forsman, C., Liang, Z., and Lindskog, S. (1992) *Biochim. Biophys. Acta* **1122**, 321–326.
33. Jackman, J. E., Merz, K. M., and Fierke, C. A. (1996) *Biochemistry* **35**, 16421–16428.

BI972081Q